5. R. P. Frankenthal and W. H. Becker, *ibid.*, **126,** 1718 (1979).
6. T. Heumann and H. S. Panesar, *Z. Phys. Chem.*, **229,** 84 (1965).
7. R. J. Chin and K. Nobe, *This Journal*, **119,** 1457 (1972).
8. A. Bengali and K. Nobe, *ibid.*, **126,** 1118 (1979).
9. J. N. Gaur and G. M. Schmid, *J. Electroanal. Chem. Interfacial Electrochem.*, **24,** 279 (1970).
10. G. Just and R. Landsberg, *Electrochim. Acta*, **9,** 817 (1964).
11. M. Pourbaix, "Atlas of Electrochemical Equilibria in Aqueous Solutions," p. 590, National Association of Corrosion Engineers, Houston, TX (1974).
12. B. E. Conway and D. M. Novak, *This Journal*, **128,** 1022 (1981).

The High Speed Electrodeposition of Sn/Pb Alloys

P. A. Kohl*

Bell Laboratories, Murray Hill, New Jersey 07974

ABSTRACT

The electrodeposition of Sn/Pb alloys and the effect of surface agents was studied in fluoboric acid solutions. Smooth, semibright deposits have been produced at current densities in excess of 800 mA/cm², approaching the mass transfer limited current. Dendrite suppression (microleveling) has been achieved by the addition of polymeric sulfactant and uniform current distributions have been obtained by the addition of lactones or other related species. When the two adsorbed species are used simultaneously the solution concentration of metal ions and the additive ratio dictate the deposition parameters. The additives have been found to be chemically more stable, less costly, and allow current densities in excess of 20× those in current commercial use.

The electrocodeposition of Sn/Pb alloys from fluoboric acid solutions was first reported in 1920 (1). Since that time, Sn/Pb alloys have seen extensive use in the electronics industry and the deposition process has slowly evolved (2). Fluoboric acid solutions are normally preferred because of the high solubility and stability of Sn(II) and Pb(II) fluoborates. The low air oxidation rate of stannous and plumbous ions and the use of soluble Sn/Pb anodes provide good stability in the high conductivity acid. Boric acid is added to prevent the hydrolysis of the fluoborate. The standard redox potentials of Sn(II) and Pb(II) are within 10 mV in this media such that codeposition is easily obtained. The high hydrogen overpotential on Sn and Pb gives the reduction process ~100% current efficiency (2). Other electrolytes such as sulfamates, pyrophosphates, and fluosilicates, have been examined; however, fluoborates remain the dominant chemistry (2).

Even though high metal ion concentrations can be obtained (*i.e.*, >1*N*), current densities of commercial systems are generally limited to 35 mA/cm² with 15-25 mA/cm² normal practice (2). The current limiting factor is the ability of additives to suppress dendritic growth and control the current distribution in geometrically restricted areas (macrothrowing power). Some of the common additives have been glue, resorcinal, nicotine, peptone, beta-naphthol, biphenyl sulfones, and ethoxy ethers (2, 3). Even with the problems of low current density and decomposition, additives of glue and peptone remain common.

In this work, the principles of high quality, high speed electrodeposition will be outlined and described for Sn/Pb deposition. Further, it will be shown that current densities in excess of 800 mA/cm² can be obtained with relatively low cost, stable additives. A versatile electrodeposition system is described where two classes of adsorbed species are used to control the rate of dendritic growth and manipulate the secondary current distribution.

Experimental

The voltammetric determinations were made using a PAR 173 potentiostat (Princeton Applied Research, Princeton, New Jersey), 179 coulometer, and 175 programmer. Positive feedback was used to compensate for solution *iR* drop. The rotating disk electrode experiments (RDE) used a Pine Instruments ASR2 rotator (Grove City, Pennsylvania) with a copper or platinum disk. There was no detectable difference between the two disk materials for Sn/Pb deposition at the current densities studied. The initial *i-V* curves were perturbed by the formation of Sn/Pb deposits on the platinum or copper electrodes, as noted. However, once surface coverage was obtained, no further effects of base metal were found.

The chemicals used in the voltammetric studies were reagent grade or analyzed to be chemically pure. The phenolphthalein (Ph) was used as a 1% solution (28 mM) in ethyl alcohol and the Triton X-100 (TX) was used at full strength. The polymer TX (C_8H_{17}-(C_6H_4)-(OCH_2CH_2)$_{9\text{-}10}$OH) was obtained from Rohm & Haas Company, Philadelphia, Pennsylvania, and the Ph (3,3-Bis(4-hydroxyphenyl)-1-(3H)-isobenzofuranone) was obtained in alcohol from Fisher Scientific Company. All solutions were deaerated for 5 min prior to use with nitrogen and a lead/lead sulfate reference electrode, whose potential was −0.65 *vs.* a saturated calomel electrode, was used. The Sn(II) and Pb(II) concentrations were analyzed polarographically in a 0.5*N* acetic acid/0.5*N* sodium acetate solution. The alloy composition was determined from the weight change per coulomb in deposition or anodic stripping. The error was less than 5%.

Results

Voltammetric behavior.—Typical voltammograms for the electrodeposition of stannous fluoborate, plumbous fluoborate, and their mixtures in fluoboric acid are shown in Fig. 1. The reduction potentials of the two species are similar and the metals are codeposited as shown in Fig. 1(c). As reduction occurs, dendritic growth is observed. This growth of crystals out from the plane of the electrode through the diffusion layer, which is higher in metal concentration, increases the surface area of the electrode. The increased area is reflected in the *i-V* curves as deviations from the convective-diffusion limiting current. The increased surface area and nonplanar electrode geometry causes the current to rise (see Fig. 1) and exceed that expected from the Levich equation for a planar surface (Eq. [1]) and produce a porous, fragile deposit as shown in Fig. 2

* Electrochemical Society Active Member.
Key words: electrodeposition, tin/lead alloys, alloy plating, solder plating.

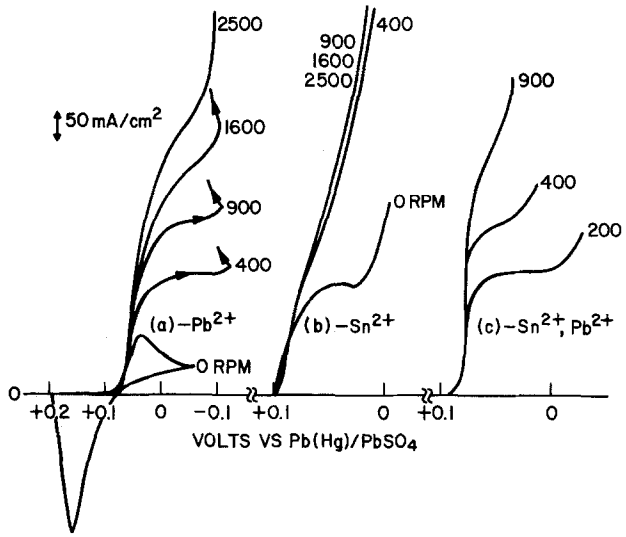

Fig. 1. Voltammograms of (a) 0.30*N* Pb^{2+}, 5*N* HBF_4; (b) 0.77*N* Sn^{2+}, 5*N* HBF_4; and (c) 0.39*N* Sn^{2+}, 0.15*N* Pb^{2+}, 6.2*N* HBF_4 at a Pt RDE. The scan rate was 10 mV/sec and the rotation speed in rpm is given.

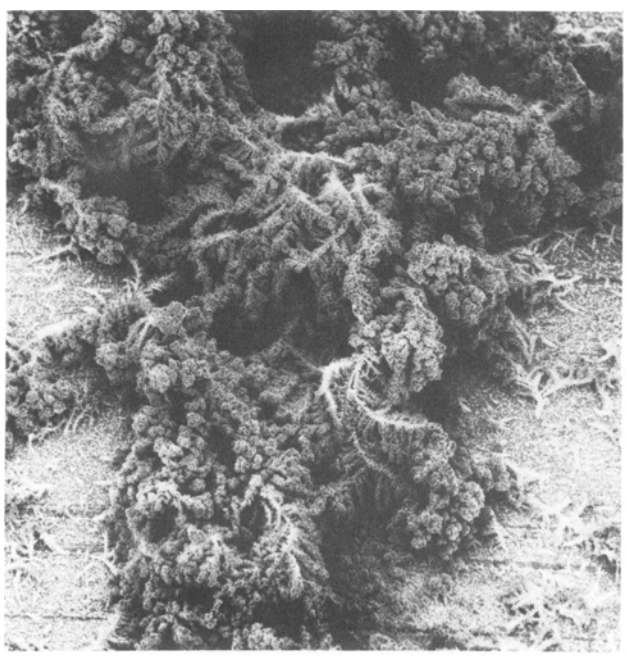

Fig. 2. Scanning electron micrograph (200× magnification) of dendritic growth produced at 30 mA/cm².

$$i_l = 0.62nFAC_T^*D^{2/3}\omega^{1/2}\nu^{-1/6} \quad [1]$$

where i_l is the limiting current, C_T^* is the total bulk concentration of Sn^{2+} and Pb^{2+}, D is the diffusion coefficient (assumed to be equal for both species), ω is the rotation speed, and ν is the kinematic viscosity. These characteristic types of deviations from i_l shown in Fig. 1 are observed at shorter times for higher rotation speed due to the increased rate of growth and decreased diffusion layer thickness.

Dendrite suppression is typically obtained in Sn/Pb deposition by maintaining low current densities and introducing additives such as glue or peptone to the system. The maximum current density obtainable without dendrite growth is limited by the ability of the additive to suppress dendrites. Although total metal concentrations in excess of 1*N* can be obtained, current densities are usually restricted to 10-30 mA/cm² (2).

The addition of Triton X-100 (TX) to the solution gives reproducible *i-V* curves with a convective-

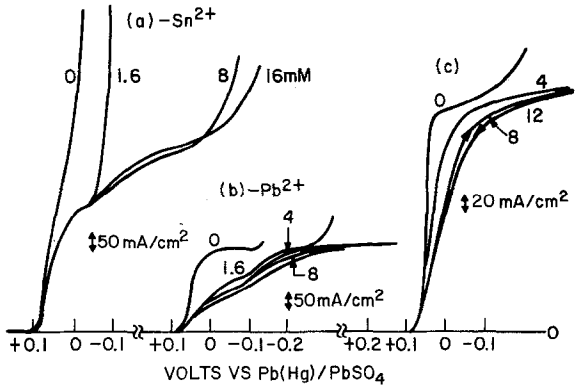

Fig. 3. Voltammograms of (a) 0.77*N* Sn^{2+}, 5*N* HBF_4; (b) 0.3*N* Pb^{2+}, 5*N* HBF_4; and (c) 0.39*N* Sn^{2+}, 0.15*N* Pb^{2+}, 6.2*N* HBF_4 at a Pt RDE rotated at 400 rpm's The concentration of Triton X-100 (in mM) is shown on each curve and the scan rate was 10 mV/sec.

diffusion limiting current plateau as shown in Fig. 3. A uniform, adherent, semibright deposit was produced at currents up to ~95% of i_l. Even at i_l, nondendritic growth was observed although the deposit was less bright. This correlation between stable *i-V* curves and fine-grained deposits was observed at all rotation speeds and concentrations used. Figure 4 is an electron micrograph of a 25 μm thick Sn/Pb deposit produced at 700 mA/cm². It should be noted that with TX, stable current-time curves (for >100 C/cm²) were observed for potentials on the rising or limiting por-

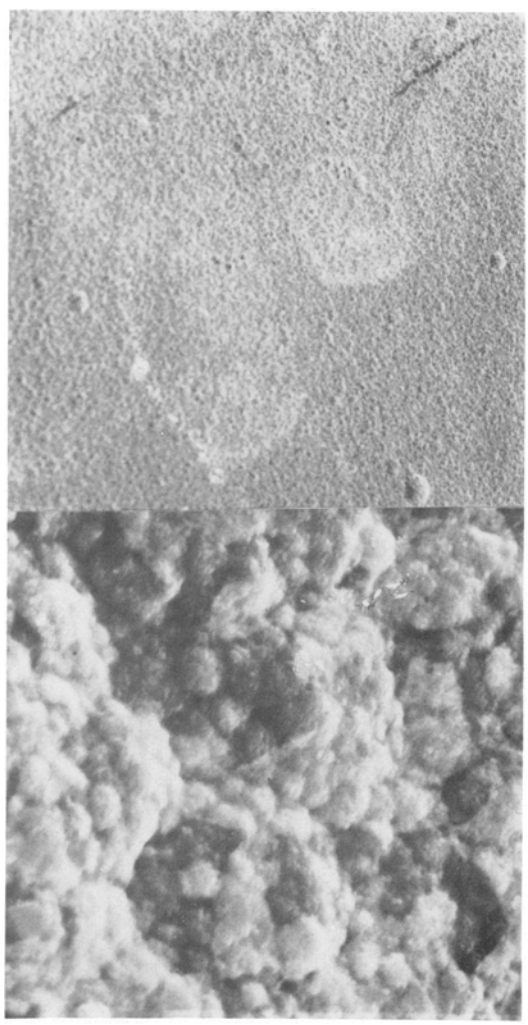

Fig. 4. Scanning electron micrograph of Sn/Pb alloy deposit at 700 mA/cm² at 200× and 8000×.

tions of the i-V curve. Conversely, dendritic growth and ascending current-time curves occurred without TX. This can also be seen in the i-V curves upon scan reversal. As seen in Fig. 1, the current continues to increase upon scan reversal with dendritic growth observed, whereas the i-V curve is retraced in Fig. 3. The prepeak observed in Fig. 1 and 3 was not found in subsequent scans or when an Sn/Pb electrode was used indicating that it is involved with the initial growth characteristics and formation of the adsorbed layer.

It has been suggested (4) that the decrease in dendritic growth is due to a poisoning of the dendrite by adsorption of the polymer. That is, dendritic growth occurs when one site or crystal face is favored over another and grows out into the diffusion layer. The adsorption of the polymer on the surface inhibits the favored growth and allows the less preferential site which is shielded from the polymer to grow. A more detailed discussion is presented in the next section.

Although current densities in excess of 800 mA/cm^2 have been obtained, with TX providing microleveling, a relatively small electrode impedance ($R_E = dE/di$) is obtained [Fig. 3(c)]. Thus the secondary current distribution will not deviate substantially from the primary current distribution in the absence of concentration polarization. The solution resistance will then be the dominant factor in the deposition profile (poor macrothrowing power) (5).

A strikingly different i-V behavior is seen in Fig. 5 upon the addition of phenolphthalein. The reduction process is greatly inhibited, as seen from the large overpotentials, while the onset of the Sn/Pb dissolution remains at the same potential. As the fractional surface coverage increases, the unperturbed area is reduced. The onset of the dendritic growth coincides with the upshoot in current and only very low current densities are obtained before dendritic growth is observed. Nontraceable i-V curves are obtained upon scan reversal. The Ph is able to suppress the growth of the Sn/Pb deposit, however, the suppression does not extend to the growth of dendrites. This large overpotential, which increases the electrode impedance, was found on lead and lead alloys but did not occur on pure tin. Generally, as the mass transfer rate is increased, dendritic growth is observed at lower potentials. This type of behavior, high electrode impedance with low threshold for dendritic growth, is similar to that found in conventional Sn/Pb deposition. The high electrode impedance of the systems, which allows the secondary current to deviate from the primary current, is limited to low current densities. An increased mass transfer rate results in dendritic and porous deposits.

The combination of the larger polymer TX (for microleveling or dendrite suppression) and the smaller Ph for increased electrode resistance (throwing power) produces a desirable effect. Figures 6-9 show the effect of the addition of Ph to a 16 mM TX solution at various metal concentrations on the i-V curve. The mol ratio of Sn to Pb was held constant and the initial slope of the i-V curves was set by the ratio of the TX and Ph while the limiting current was determined by the bulk metal concentration. Smooth, adherent deposits were produced at current densities up to ~90% of i_l (5). At lower metal concentrations the prepeak becomes more pronounced (Fig. 9); however, upon scan reversal or initial use of an Sn/Pb electrode, no peak was observed as mentioned previously.

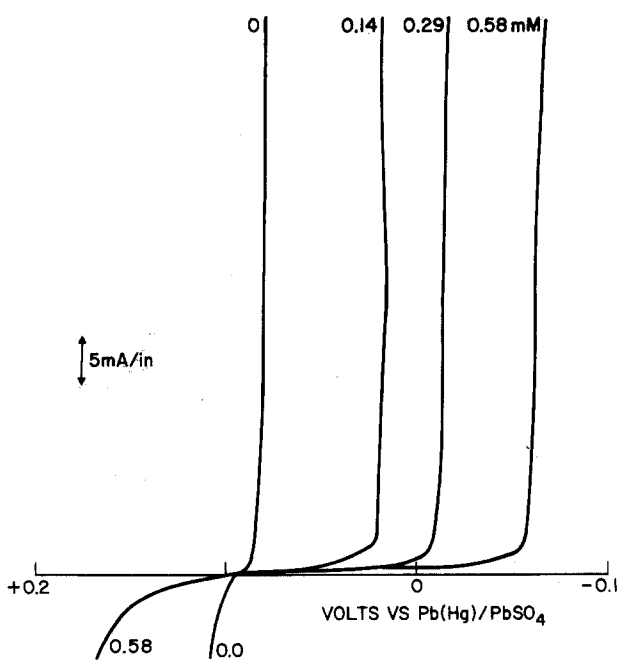

Fig. 5. Voltammogram of 0.39N Sn^{2+}, 0.15N Pb^{2+}, in 6.2N HBF_4 at Pt RDE. The rotation rate was 200 rpm and scan rate 5 mV/sec. The concentration of phenolphthalein (mM) is shown.

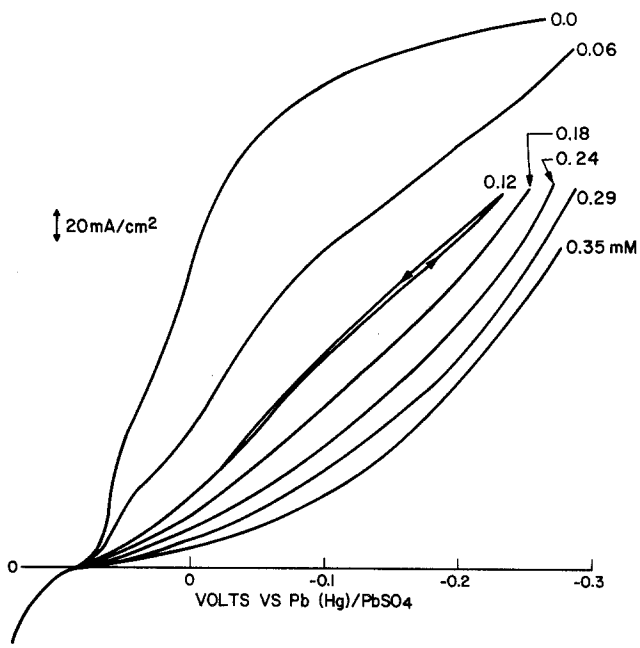

Fig. 6. Voltammogram of a 0.58N Sn^{2+}, 0.23N Pb^{2+}, 5N HBF_4, and 16 mM Triton X-100 solution with phenolphthalein concentration (mM) shown. A Pt disk electrode at 400 rpm's was used and the scan rate was 10 mV/sec.

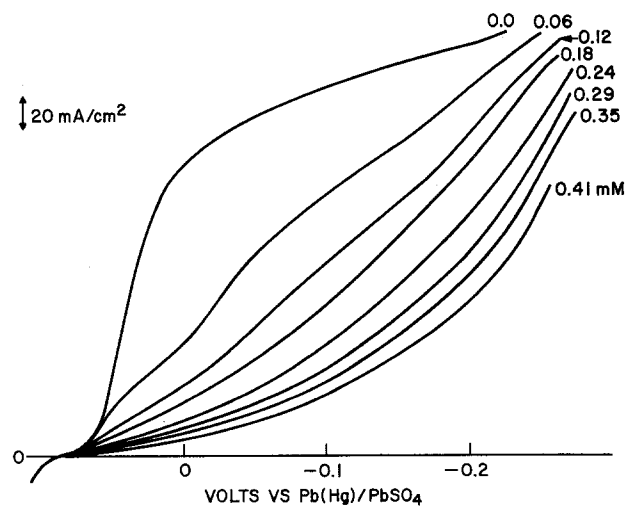

Fig. 7. Same as Fig. 6 except 0.38N Sn^{2+} and 0.15N Pb^{2+}

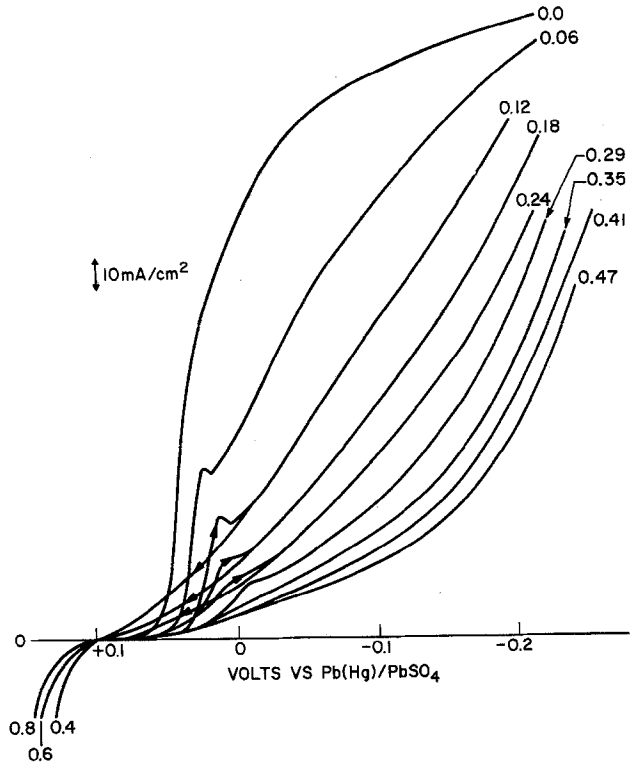

Fig. 8. Same as Fig. 6 except 0.27*N* Sn^{2+} and 0.10*N* Pb^{2+}

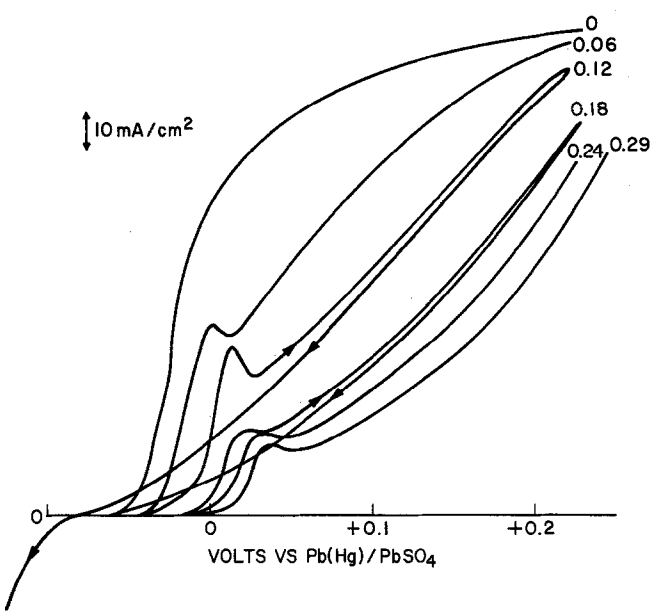

Fig. 9. Same as Fig. 6 except 0.19*N* Sn^{2+} and 0.075*N* Pb^{2+}

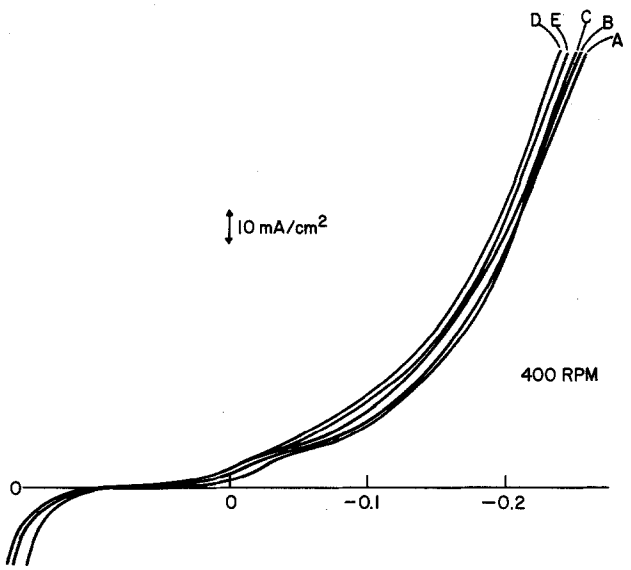

Fig. 10. Voltammogram of 0.27*N* Sn^{2+} and 0.10*N* Pb^{2+} with a constant mol ratio of TX/Ph = 40: (a) TX = 8 mM, Ph = 0.20; (b) TX = 24 mM, Ph = 0.6 mM; (c) TX = 32 mM, Ph = 0.81 mM; (d) TX = 48 mM, Ph = 1.22 mM; and (e) TX = 80 mM, Ph = 2.0 mM. The rotation speed was 400 rpm and scan rate 10 mV/sec.

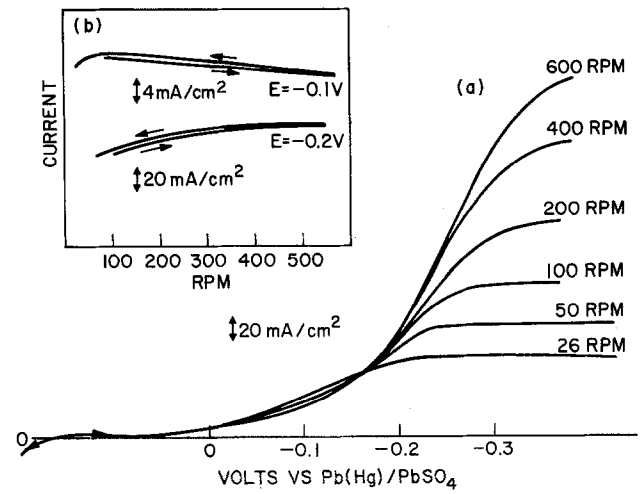

Fig. 11. (a) Voltammogram of a 0.27*N* Sn^{+2}, 0.10*N* Pb^{+2}, 5*N* HBF_4, 16 mM TX, and 0.40 mM Ph solution at a Pt RDE. (b) Current density *vs.* RPM at two potentials from part a.

Figure 10 illustrates how the shape of the *i-V* curve is determined by the mol ratio of the two additives and not by the absolute concentrations (within limits) as is observed with one component systems (*i.e.*, Ph alone). In Fig. 10, the concentration of the additives is changed by 10× while little change is observed at 40:1 TX:Ph.

The effect of mass transfer rate is demonstrated in Fig. 11(a) where i_l is determined by the mass transfer rate (rotation speed). An increasing rotation speed has a reverse effect on the rising portion of the curve [Fig. 11(b)]. Increasing the mass transfer rate decreases the current density at −0.1V. At potentials less than −0.2V the more usual behavior of concentration polarization and mass transfer rate is observed, as described by Eq. [1].

The role the additives play in the deposition process has been found to be time independent. Figure 12(a) shows the consistency of the deposit composition as the solution is aged with a 2.6 mol ratio consumable anode at ~20 mA/cm². After greater than 540,000 C/liter, which corresponds to over 8 solution turnovers, the deposit was smooth and adherent. The total amount of TX and Ph added was 51 and 0.61 mM, respectively. The change in the *i-V* curves are shown in Fig. 12(b). This shows that the rate of decomposition and dragout of the additives (> 6000 cm² total area) is small in this case. For other situations where the total area will be many times greater (thinner deposit) the dragout may increase. The decrease in i_l for curves 2 and 3 of Fig. 12(b) is due to the slow formation of the insoluble Sn(IV) and Pb(IV) species at the anode (slightly less than 100% efficient) which decreases the total metal content. A 30% replenishment in metal ion content was made in curve 4.

The function of the additives is believed to be due to their adsorption on the electrode surface as discussed in the next section. The difference in size, solubility, and degrees of freedom in the polymer chain produces the two different effects. It has been found that the same effects can be obtained with other re-

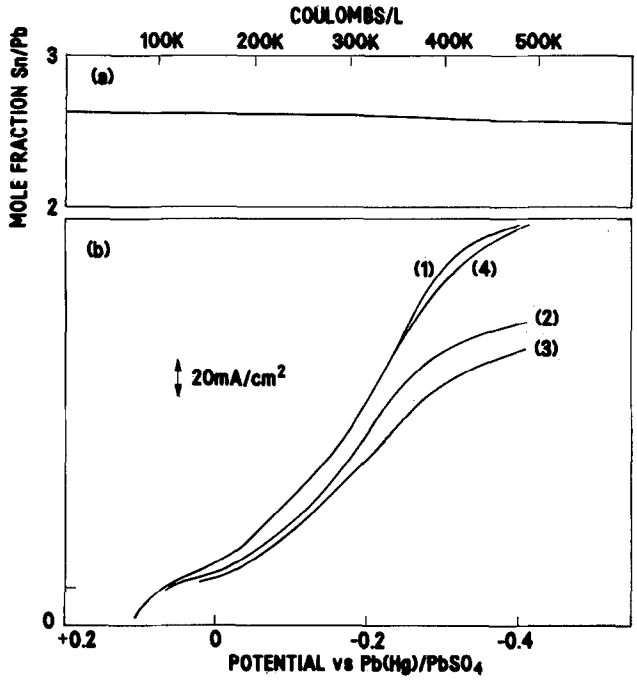

Fig. 12. (a) Mol ratio of Sn/Pb deposit *vs.* C/liter from a 0.27*N* Sn^{2+} and 0.10*N* Pb^{2+} solution with total TX = 51 mM and Ph 0.61 mM. (b) Voltammograms at various points from part a. Curves 1, 2, 3, and 4 are for 0, 120 K, 400 K, and 540 K C/liter, respectively. The rotation rate was 400 rpm and the scan rate was 10 mV/sec.

lated compounds. For example, the size at the polymer chain can be varied from 5 to 30 units with similar dendrite suppression. Other related phthaleins, heterocyclics, have been found to produce similar effects when used in conjunction with TX. For example, phenol red (I), α-naphthalphthalein (II), and 2-benzoxazolinone (III) increase the electrode impedance in a manner analogous to phenolphthalein (IV).

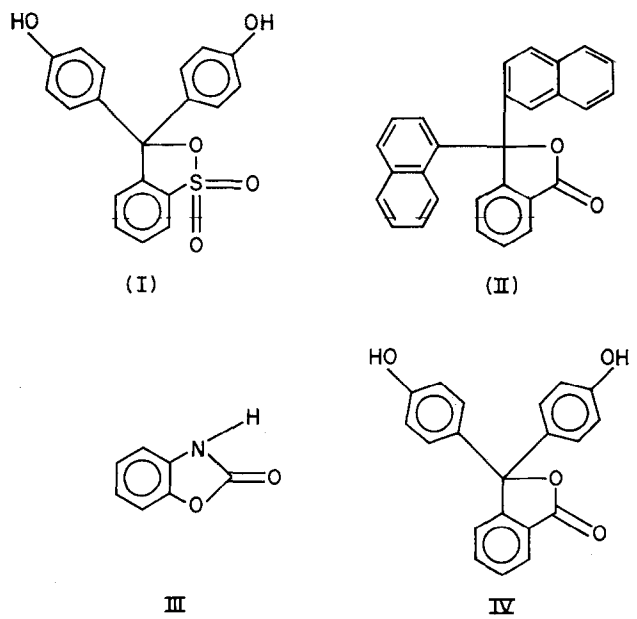

The stability in the *i-V* curves is demonstrated in Fig. 12(b) where the equivalents of charge passed are in excess of 10,000 times the mols of phenolphthalein present. This is contrary to the decomposition or co-deposition of conventional additives (2). It has been shown (6-8) that Ph and related compounds in their acid form (as a closed ring lactone) are not reducible in aqueous solutions; however, at a mercury electrode the lactone undergoes a ring opening and is reduced. The reduction of Ph was not observed in fluoboric acid solutions [without Sn(II) or Pb(II)] at an Sn/Pb electrode although the hydrogen overpotential was not as great as with mercury.

Although the redox potential for Sn(II) and Pb(II) are within 10 mV in HBF_4, lead is the more noble metal and the reduction of Pb(II) is favored at currents less than i_l (2). Figure 13(a) shows a typical composition *vs.* current density relation at a fixed mass transfer rate. As the current approaches i_l the deposit composition approaches the stoichiometric solution ratio [*i.e.*, 2.6 in Fig. 13(a)]. The activity of Pb and Sn is reversed from that shown in Fig. 3 for the separate metals, where the Pb current rose more slowly than Sn.

The endpoint requirement for Sn/Pb deposit composition, current density, and mass transfer rate dictates the solution composition and metal ratio [as shown for example in Fig. 13(a)]. However, the use of soluble anodes of the desired deposit composition ensures that correct solution ratio will be obtained. Assuming a 100% anode and cathode efficiency, the metal ratio in solution will change so that the deposit composition will be the same as the soluble anode. The change in deposit composition can be calculated as follows. If the current $i_x(t)$, for a species x at time t, is directly related to the concentration of x such as for the mass transfer limited current then

$$\frac{i_x(t)}{nFA} = m_o C_x(t) \qquad [2]$$

where m_o is the mass transfer coefficient (assumed to be equal for Sn and Pb) and $C_x(t)$ is the bulk concentration of species x at time t in mol/cm³. The volume of the electrode double layer is assumed to be negligible. Then, under constant current electrolysis with a soluble anode (mol ratio of tin to lead, M_x), the change in concentration of x is given by

$$\frac{dC_x(t)}{dt} = \frac{-m_o A}{V} C_x(t) + \frac{M_x i_T}{nFV} \qquad [3]$$

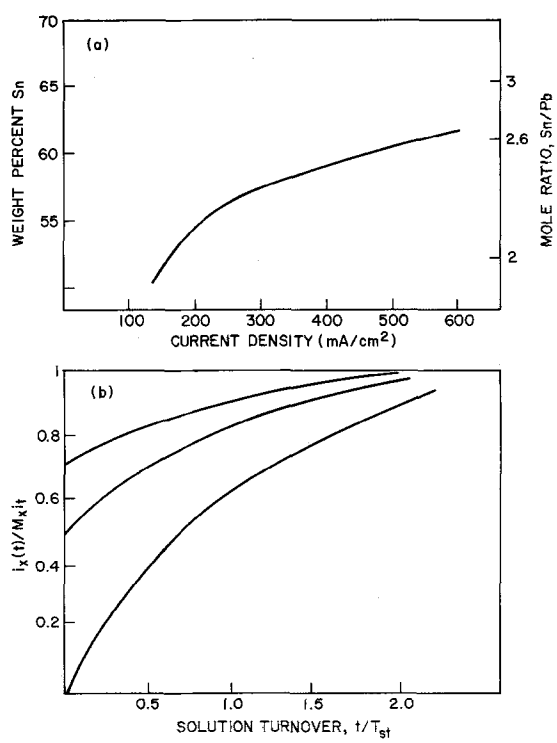

Fig. 13. (a) Change in deposit composition *vs.* current density for a 0.38*N* Sn^{2+} and 0.15*N* Pb^{2+} solution. (b) Change in partial current *vs.* solution turnovers with soluble anodes.

where i_T is the total current [sum of all $i_x(t)$] and V is the solution volume. Upon integration the deposition current going to species x at time t is

$$i_x(t) = M_x i_T(1 - \exp(-m_o At/V)) + i_x(0)\exp(-m_o At/V) \quad [4]$$

Further, V/m_oA can be defined as the time, T_{st}, to electrolyze the total metal content within the solution under constant current i_T (one solution turnover)

$$i_x(t) = M_x i_T(1 - \exp(-t/T_{st})) + i_x(0)\exp(-t/T_{st}) \quad [5]$$

Figure 13(b) shows in dimensionless time, t/T_{st}, the change in the ratio of the cathode current $i_x(t)$ to the anode current, $M_x i_T$, for various values of $i_x(0)$. If the cathode deposit differs from the anode composition $|i_x(0)/M_x i_T \neq 1|$ then the solution composition will change until unity is obtained. For example, if 60/40 weight percent Sn/Pb anodes were used and the initial deposit was 39/61 $|i(0)M_{Sn}/i_T = 0.7|$ then after ~0.7 solution turnovers the deposit would be 50/50.

Discussion

The Sn/Pb deposition parameters from fluoboric acid solutions must be altered to give an acceptable metallurgical deposit. Adsorption of solution species changes the reduction kinetics and mechanism and is the most common method of producing uniform Sn/Pb deposits. Each of the two species, TX and Ph, produces strikingly different effects on the reduction of the metal ions. The addition of < 1 mM Ph to a > 0.5M M^{2+} solution increases the reaction overpotential (R_E) while having little effect on the rate of dendritic growth. Addition of TX has only a minor effect on the i-V curve but provides uniform deposition rates to an equipotential surface. The addition of an adsorbable organic compound can affect a reaction in several ways. The adsorbed species must desorb to allow the adatom and subsequent lattice formation steps to take place (4). Further, if the adsorbed species affects the double layer structure and properties then the metal-solution potential may be reduced so that the potential felt by the metal ions is reduced (9, 10). The remaining potential drop would occur across the diffuse layer, ϕ_2. The decrease in potential would slow the velocity of the reaction.

Because of the differences in solubilities, size, and structures of the two adsorbed species, they affect the reduction process on different scales. The smaller more rigid species Ph, which is less soluble, adsorbs over the entire surface and decreases the rate of reaction uniformly. The larger surfactant, TX, whose polar end is soluble and nonpolar tail can form micelles, inhibits the growth of dendrites or peaks protruding into the double layer but does not inhibit the entire planar surface as effectively. Thus the leveling effect is greatest on the peaks (5). It was concluded (11) that the rate-limiting step for the electrodeposition of tin from acid stannous solutions is probably charge transfer through a layer of adsorbed organic molecules. This inhibition of the dendrites then allows the less favored sites to grow. Thus the Ph acts as a macroleveling agent (high R_E) while the TX acts as a microleveling agent. The data indicate that the relative concentration of two additives in solution sets the surface ratio and relative effect of each species.

To balance these two effects the ratio of the two species is varied. Figure 14 shows how the electrode impedance (R_E) varies over the first 100 mV of the cathodic i-V scan. A high value of R_E/R_S produces macrothrowing power with a uniform secondary current distribution, where R_S is the solution resistance. While a minimum slope (*i.e.*, limiting current plateau) affords the highest R_E/R_S ratio, it is difficult to maintain in a controlled current mode. Thus it is desirable to have a linear i-V behavior with a minimum slope to produce uniform throwing power at all current densities. The limiting current is determined by the mass transfer rate and solution concentration, Eq. [1]. Thus the ratio of Ph/TX, solution concentration, and mass transfer rate can be set to produce the desired current density and throwing power.

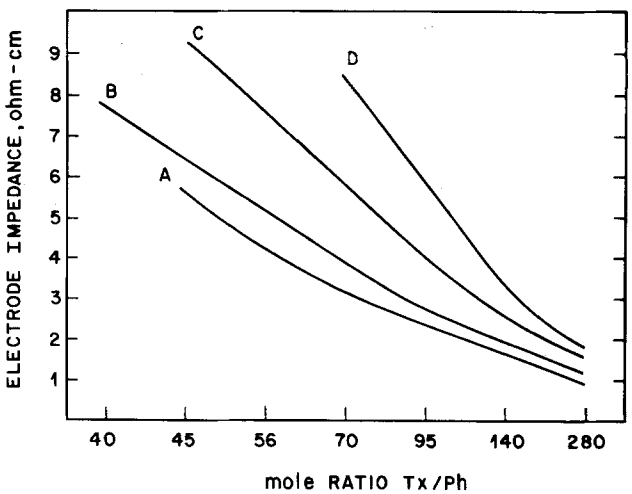

Fig. 14. Electrode impedance (R_E) as measured from the first 100 mV of the i-V curves for (a) 0.58N Sn^{2+}, 0.23N Pb^{2+}; (b) 0.38N Sn^{2+}, 0.15N Pb^{2+}; (c) 0.27N Sn^{2+}, 0.10N Pb^{2+}; and (d) 0.19N Sn^{2+}, 0.075N Pb^{2+}. The solution resistances for the four curves are 2.7, 2.0, 1.8, and 1.7 Ω cm, respectively.

Conclusions

The Sn/Pb electrodeposition parameters can be chemically manipulated to give adherent, semibright deposits at currents in excess of 800 mA/cm². The inability of a single species to control the two modes of growth (increased rate of nucleation and dendritic growth), has led to the use of additives that are more stable than previously used compounds. Furthermore, it has been shown that the deposition characteristics are independent of the absolute amount of the additives and dependent only on their mol ratio.

Manuscript submitted March 11, 1981; revised manuscript received *ca.* Dec. 7, 1981.

Any discussion of this paper will appear in a Discussion Section to be published in the December 1982 JOURNAL. All discussions for the December 1982 Discussion Section should be submitted by Aug. 1, 1982.

Publication costs of this article were assisted by Bell Laboratories.

REFERENCES

1. J. F. Groff, U.S. Pat. 1,364,051 (1920).
2. A. Brenner, "Electrodeposition of Alloys," Academic Press, New York (1963).
3. (a) I. Rajagopal and K. S. Rajam, *Metal Finish.*, **76**, 43 (1978); (b) *ibid.*, **77**, 37 (1979); (c) *ibid.*, **76**, 51 (1978).
4. J. A. Harrison and H. R. Thirsk, in "Electroanalytical Chemistry," Vol. 5, A. J. Bard, Editor, Marcel Dekker, New York (1971).
5. N. Ibl, Ph. Javet, and F. Stakel, *Electrochim. Acta*, **17**, 733 (1972).
6. I. M. Kolthoff and D. J. Lehmicke, *J. Am. Chem. Soc.*, **20**, 1879 (1948).
7. M. M. Ghoneim, A. M. Khalil, and A. M. Hassanein, *Electrochim. Acta*, **21**, 623 (1979).
8. M. M. Ghoneim and M. A. A. Ashy, *Can. J. Chem.*, **57**, 1294 (1979).
9. J. Lipkowski and Z. Galus, *J. Electroanal. Chem. Interfacial Electrochem.*, **98**, 91 (1978).
10. R. Parsons, *ibid.*, **21**, 35 (1969).
11. S. Meibuhr, E. Yeager, A. Kozawa, and F. Hovorka, *This Journal*, **110**, 190 (1963).